Supporting Information

Non-Monotonic Plasmonic Alignment Governed by Liquid-Crystalline DNA Hydrogel Networks

Juri Kim[†a], Soon Mo Park[†b], Mingeun Kim[c], Hee Seong Yun[a,d], Jin Suk Myung[c], Woo Jin Choi[c] and Dong Ki Yoon[a,d]*

†J. Kim and S.M. Park contributed equally to this paper

[a] Department of Chemistry, Korea Advanced Institute of Science and Technology, Daejeon 34141, Republic of Korea

[b] Department of Chemical and Biomolecular Engineering, Cornell University, Ithaca, 14853, USA

[c] Digital Chemistry Research Center, Korea Research Institute of Chemical Technology (KRICT), Daejeon, 34114, Republic of Korea

[d] GIST InnoCORE AI-Nano Convergence Initiative for Early Detection of Neurodegenerative Diseases, Gwangju Institute of Science and Technology, 61005 Gwangju, Republic of Korea

*To whom correspondence should be addressed.

E-mail: : nandk@kaist.ac.kr (D. K. Yoon)

This PDF file includes:
Fig. S1 to S20

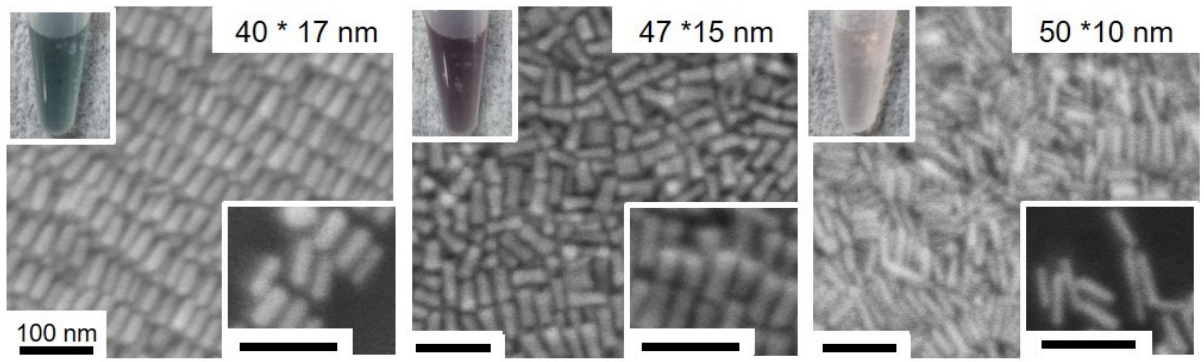

Fig. S1 SEM images of gold nanorods (GNRs) with varying aspect ratios. Insets show the solution images corresponding GNR colloidal dispersions. All scale bars represent 100 nm.

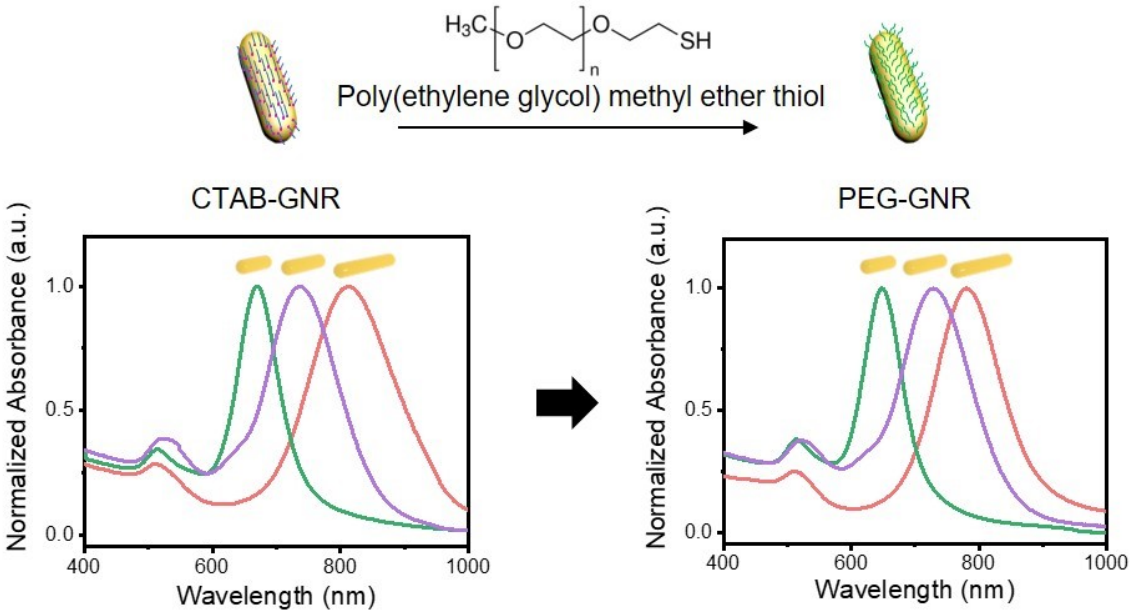

Fig. S2 Schematic representations of gold nanorods with different surface functionalizations (left: Cetrimonium bromide (CTAB); right: thiolated polyethylene glycol (PEG–SH)) and their corresponding normalized UV–Vis–NIR absorption spectra.

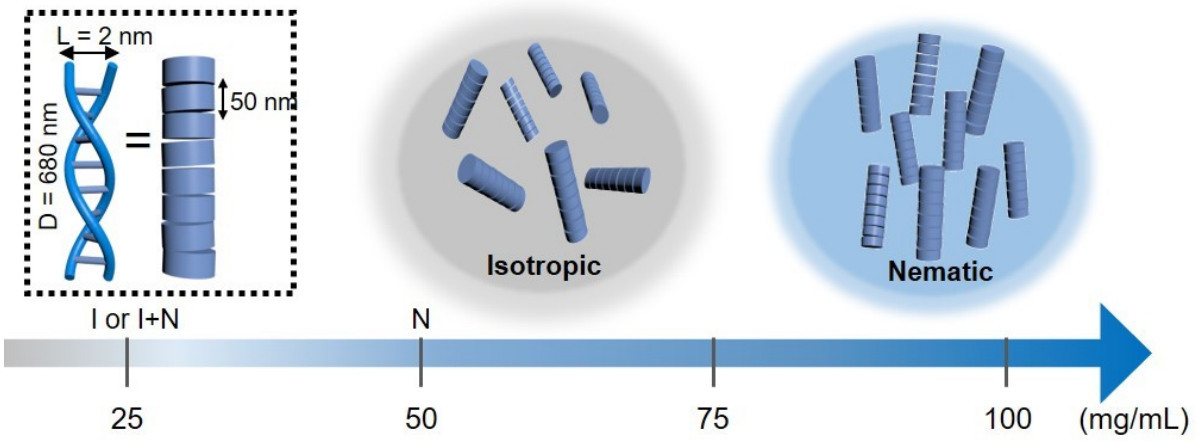

Fig. S3 Schematic illustration of liquid crystal phases of the salmon DNA depending on concentration.

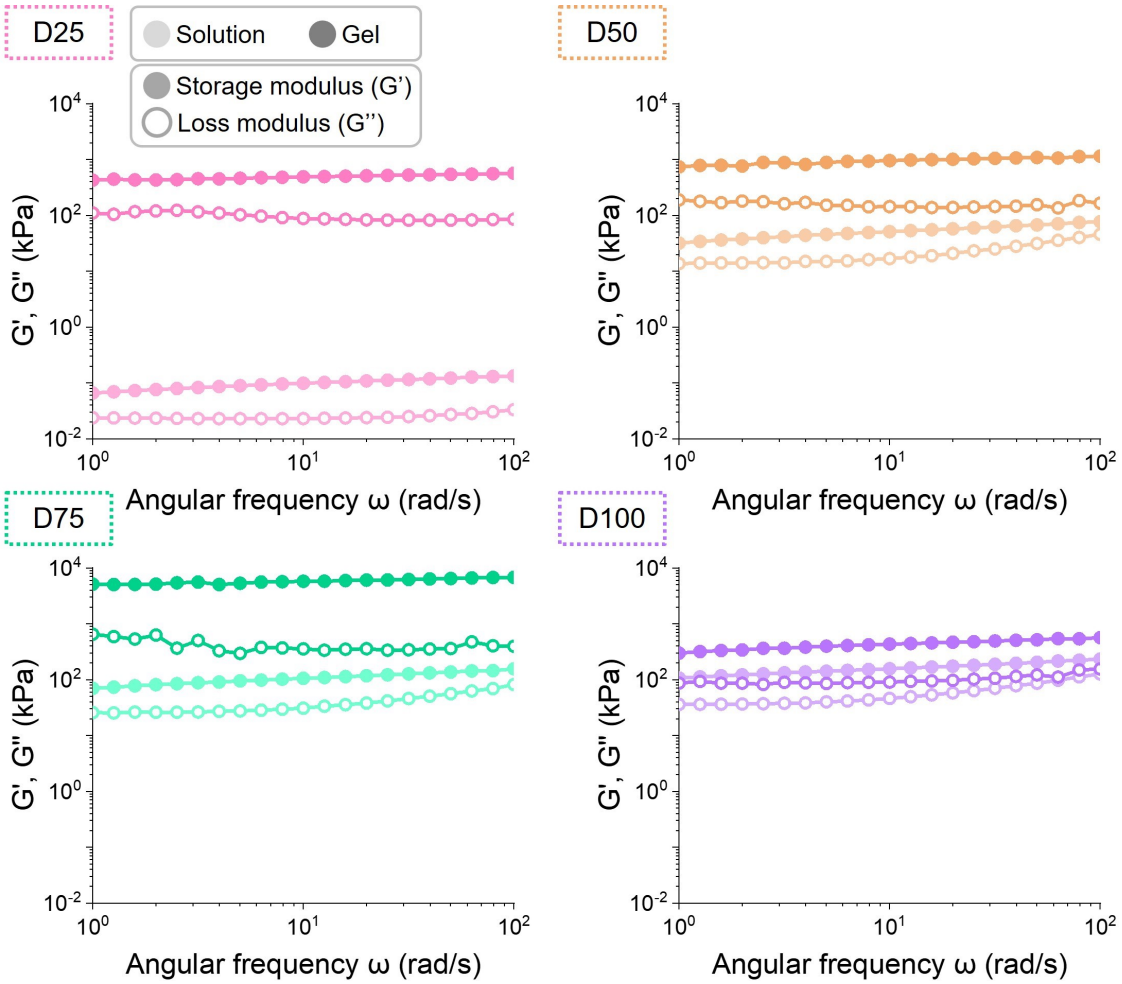

Fig. S4 Frequency sweep of DNA – GNR solution and gel depending on concentration of DNA.

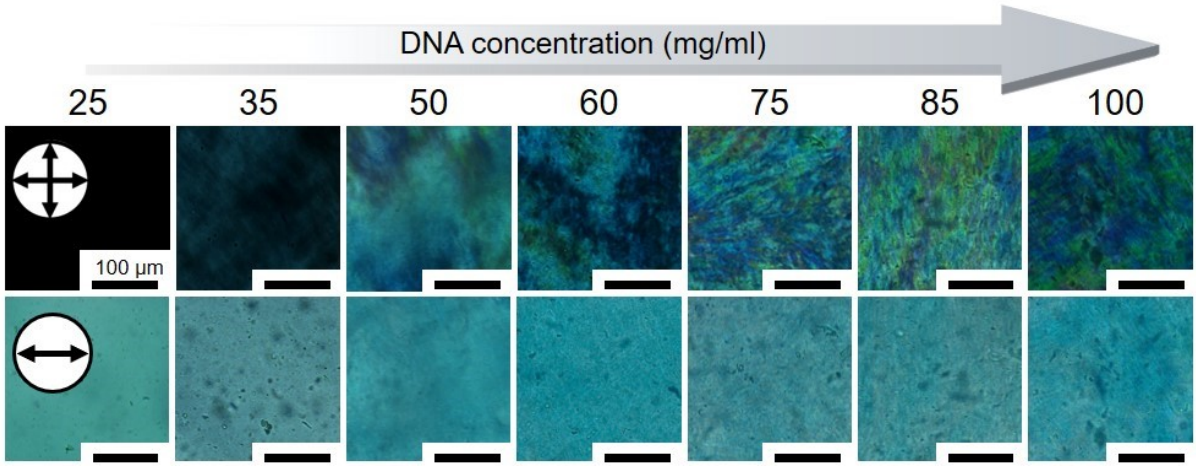

Fig. S5 Polarized optical microscopy images of DNA – GNR solutions at varying DNA concentrations. The top row shows crossed-polarized images (C-POM), while the bottom row shows linearly polarized images (L-POM). All scale bars indicate 100 µm.

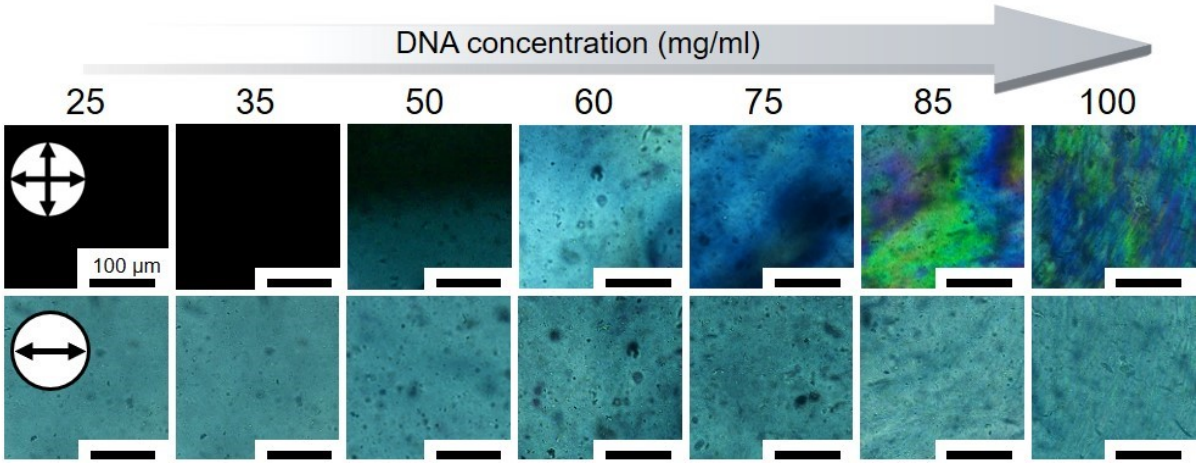

Fig. S6 Polarized optical microscopy images of as-prepared DNA–GNR hydrogels at more finely divided DNA concentrations. The top row shows crossed-polarized images (C-POM), while the bottom row shows linearly polarized images (L-POM). All scale bars indicate 100 μm.

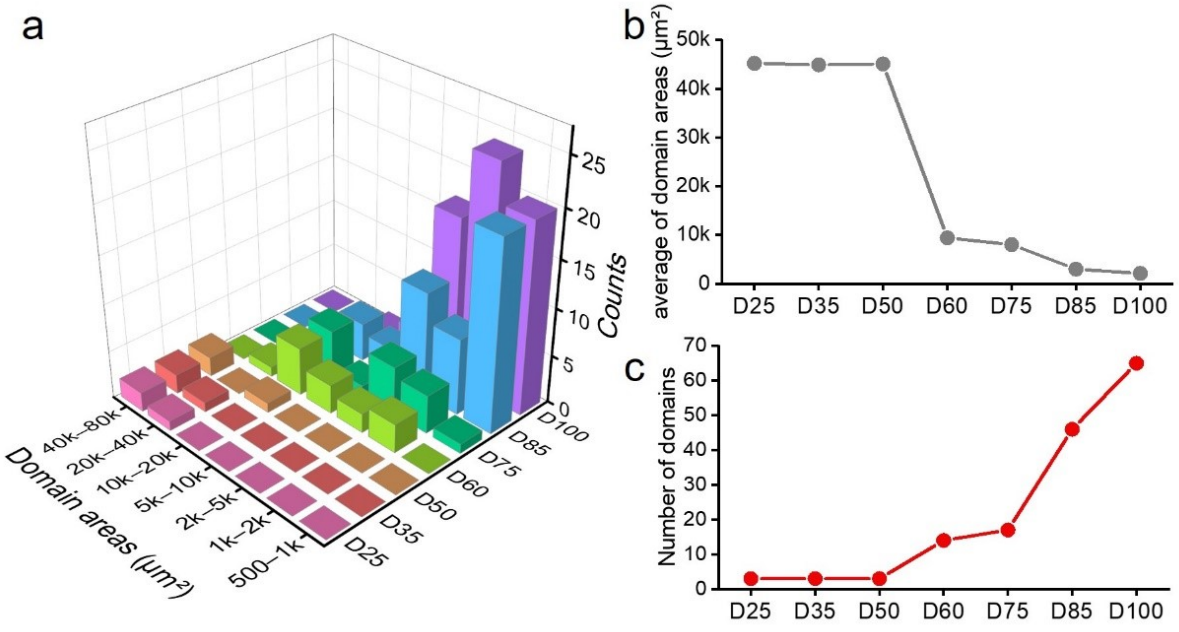

Fig. S7 Polarized optical microscopy (POM) images of DNA gels acquired over an area of 1.4 × 10^5 μm² were analyzed to quantify domain statistics at different DNA concentrations. (a) Histograms of domain area distributions, (b) average domain area, and (c) total number of domains as a function of DNA concentration.

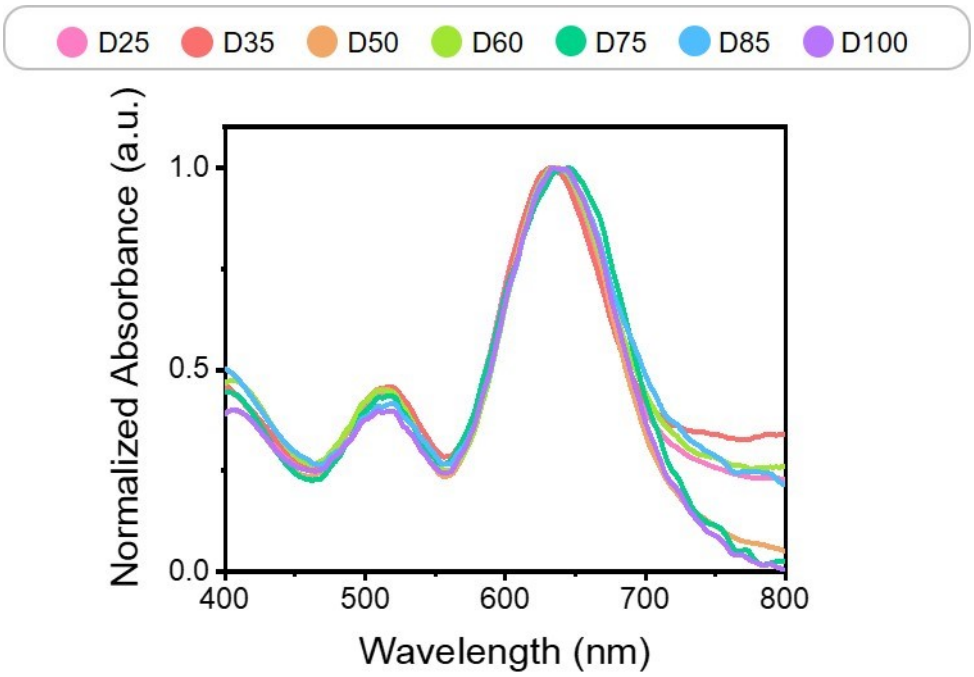

Fig. S8 UV–Vis absorption spectra of as prepared DNA–GNR hydrogels at various DNA concentrations.

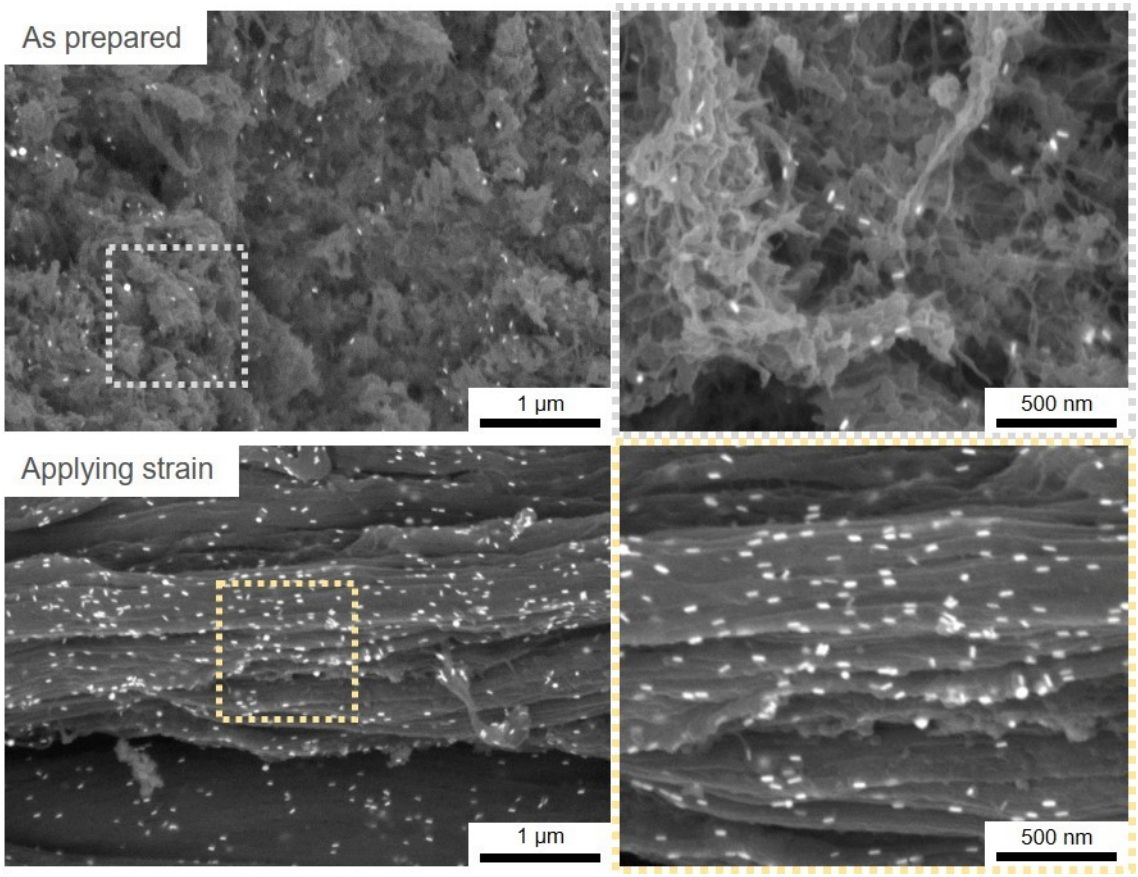

Fig. S9 SEM images showing the internal structure of the DNA–GNR hydrogels: (a) as prepared (without strain) and (b) after applying tensile strain. Right panels show magnified views of the regions indicated by dashed boxes in the left images.

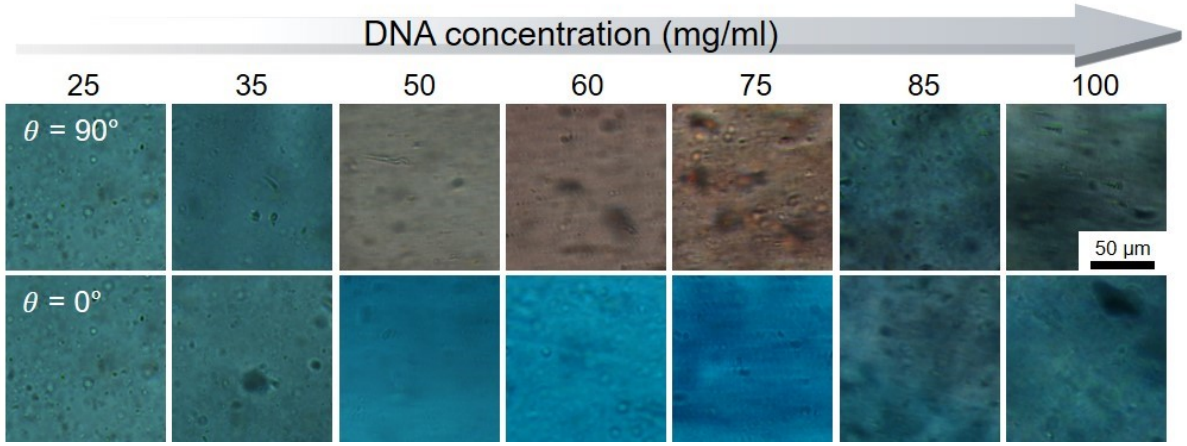

Fig. S10 Polarization-dependent optical images of the DNA–GNR hydrogels at a strain level just before fracture, illustrating color variations under different polarization directions.

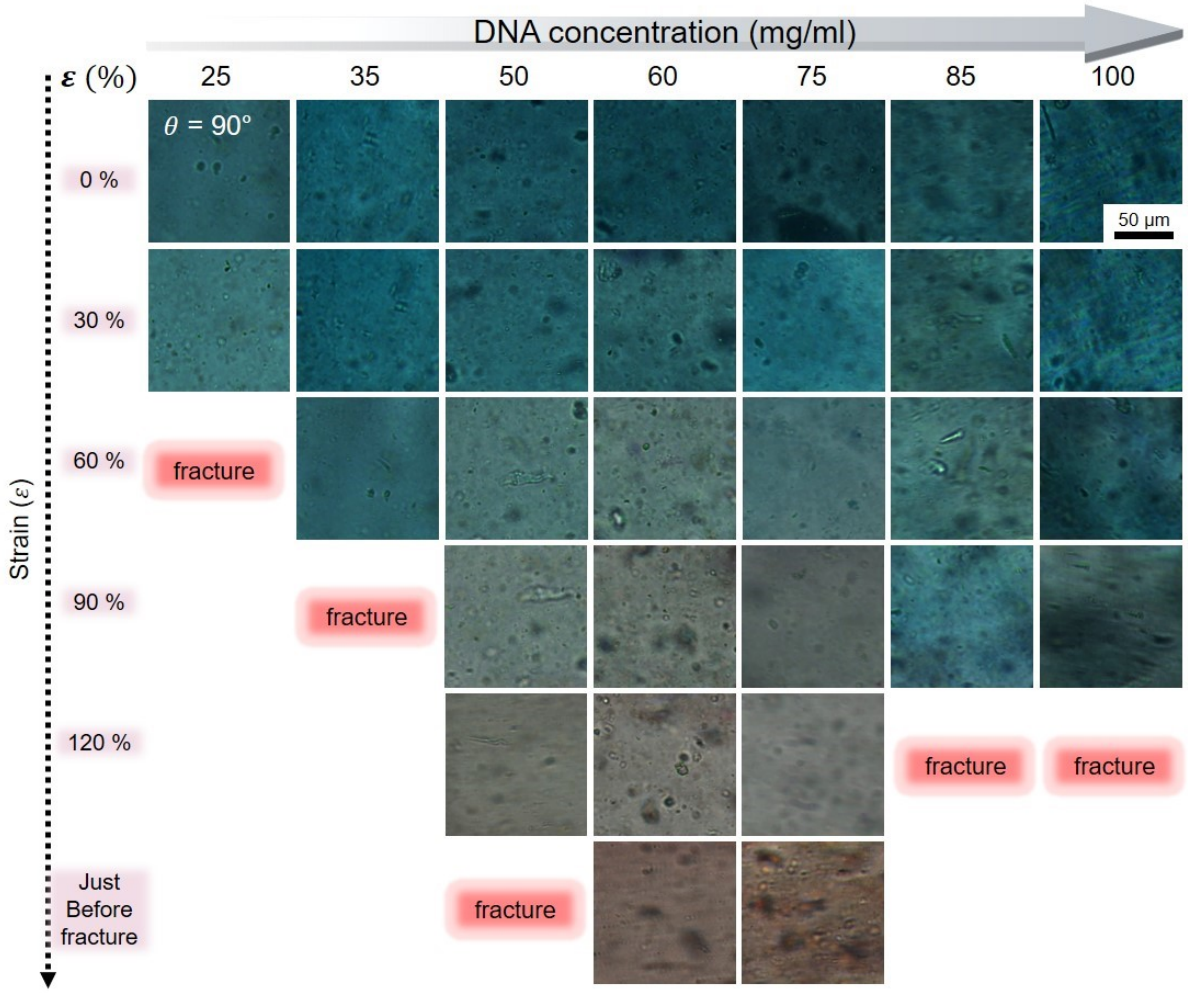

Fig. S11 Polarization-dependent optical images of DNA–GNR hydrogels at various DNA concentrations and strain levels. Images were taken just before fracture under L-POM, with the polarization direction oriented perpendicular to the stretching direction. The black double-headed arrow indicates the polarization direction, and the dashed arrow indicates the direction of applied strain. The fracture points are labeled accordingly.

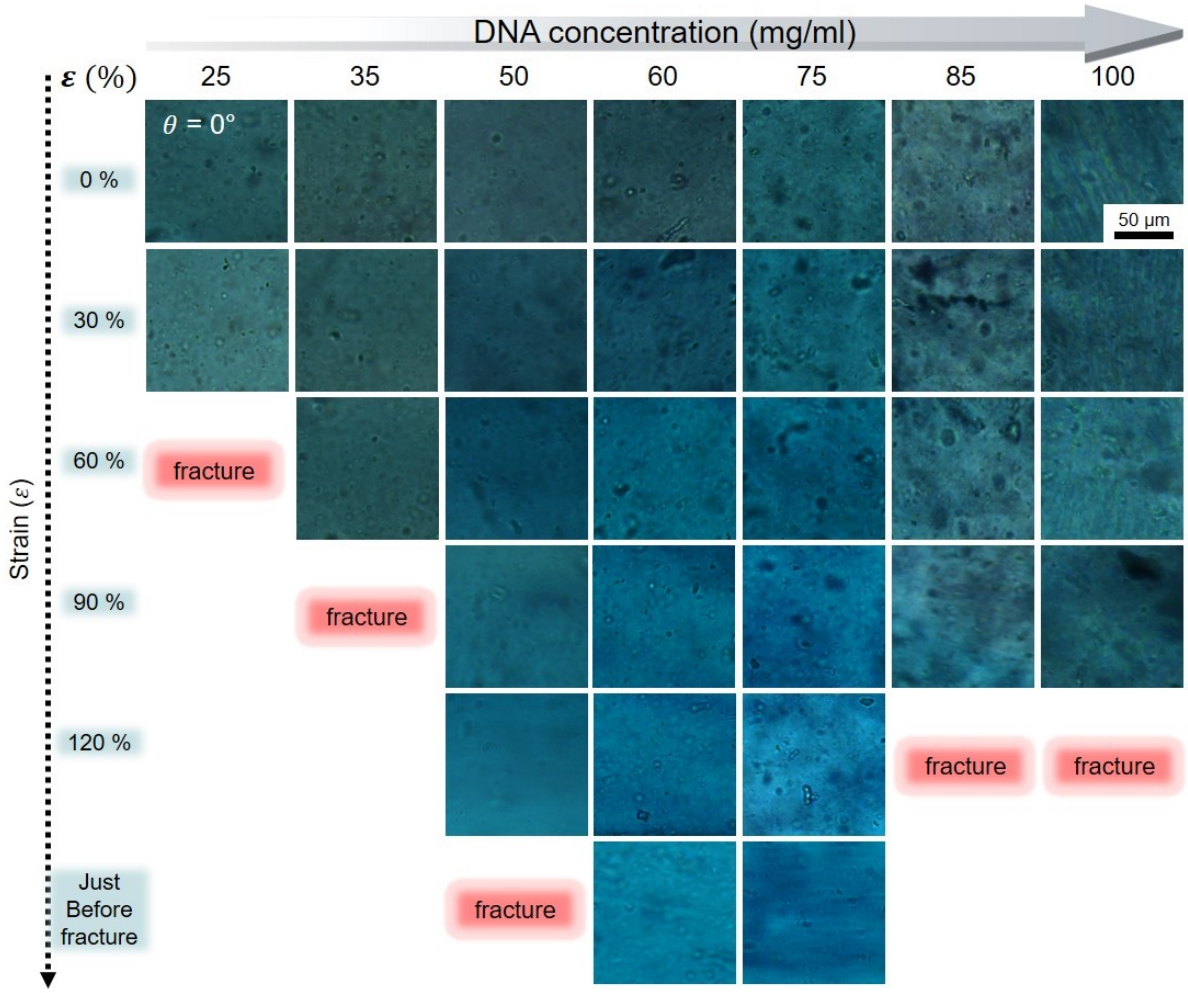

Fig. S12 Polarization-dependent optical images of DNA–GNR hydrogels at various DNA concentrations and strain levels. Images were taken just before fracture under L-POM, with the polarization direction oriented parallel to the stretching direction. The black double-headed arrow indicates the polarization direction, and the dashed arrow indicates the direction of applied strain. The fracture points are labeled accordingly.

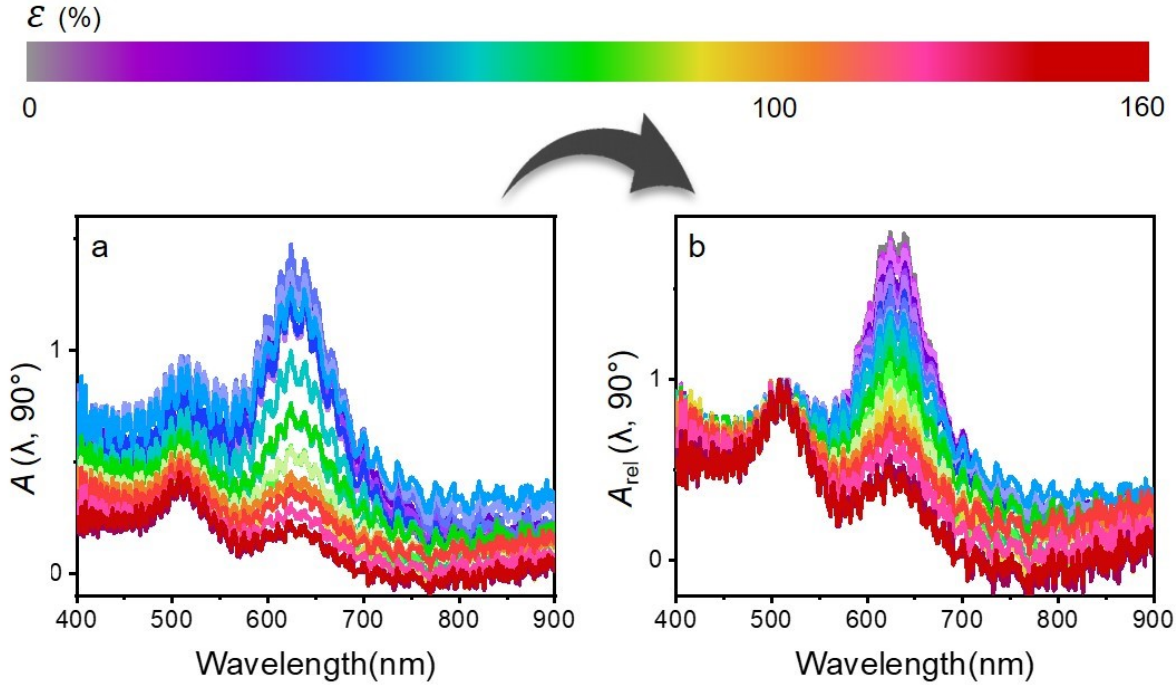

Fig. S13 (a) Polarized absorbance spectra $A(\lambda, 90°)$ of the 75 mg/mL DNA–GNR hydrogel measured as a function of applied strain, with polarization perpendicular to the strain axis. (b) Corresponding relative absorbance spectra $A_{rel}(\lambda, 90°)$, obtained by normalizing each spectrum in a) to the peak maximum of the transverse-mode absorbance $A_{trans}(90°)$, to highlight strain-dependent spectral evolution.

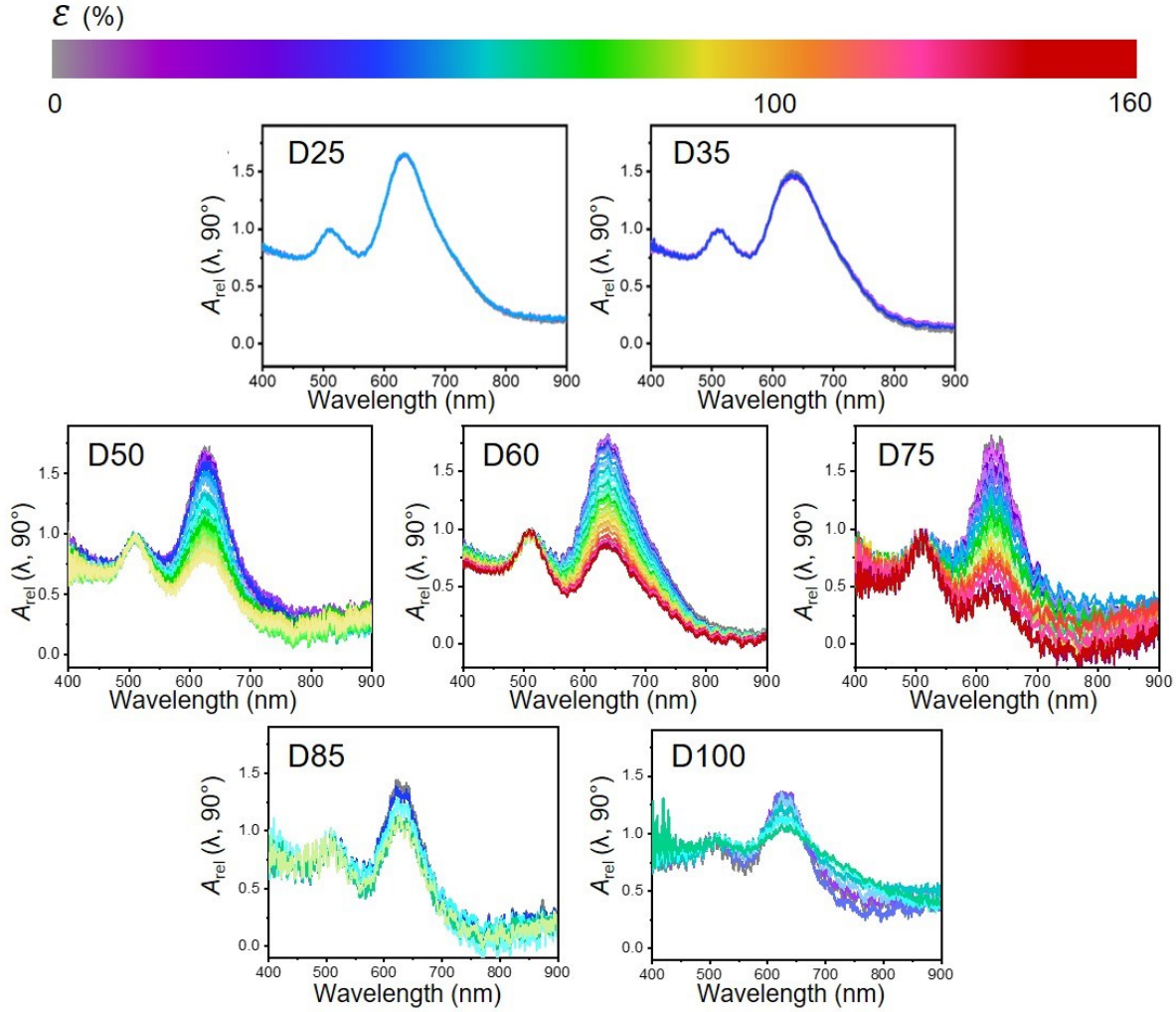

Fig. S14 Comparison of the strain-dependent relative absorbance spectra $A_{rel}(\lambda, 90°)$ of DNA–GNR hydrogels at varying DNA concentrations.

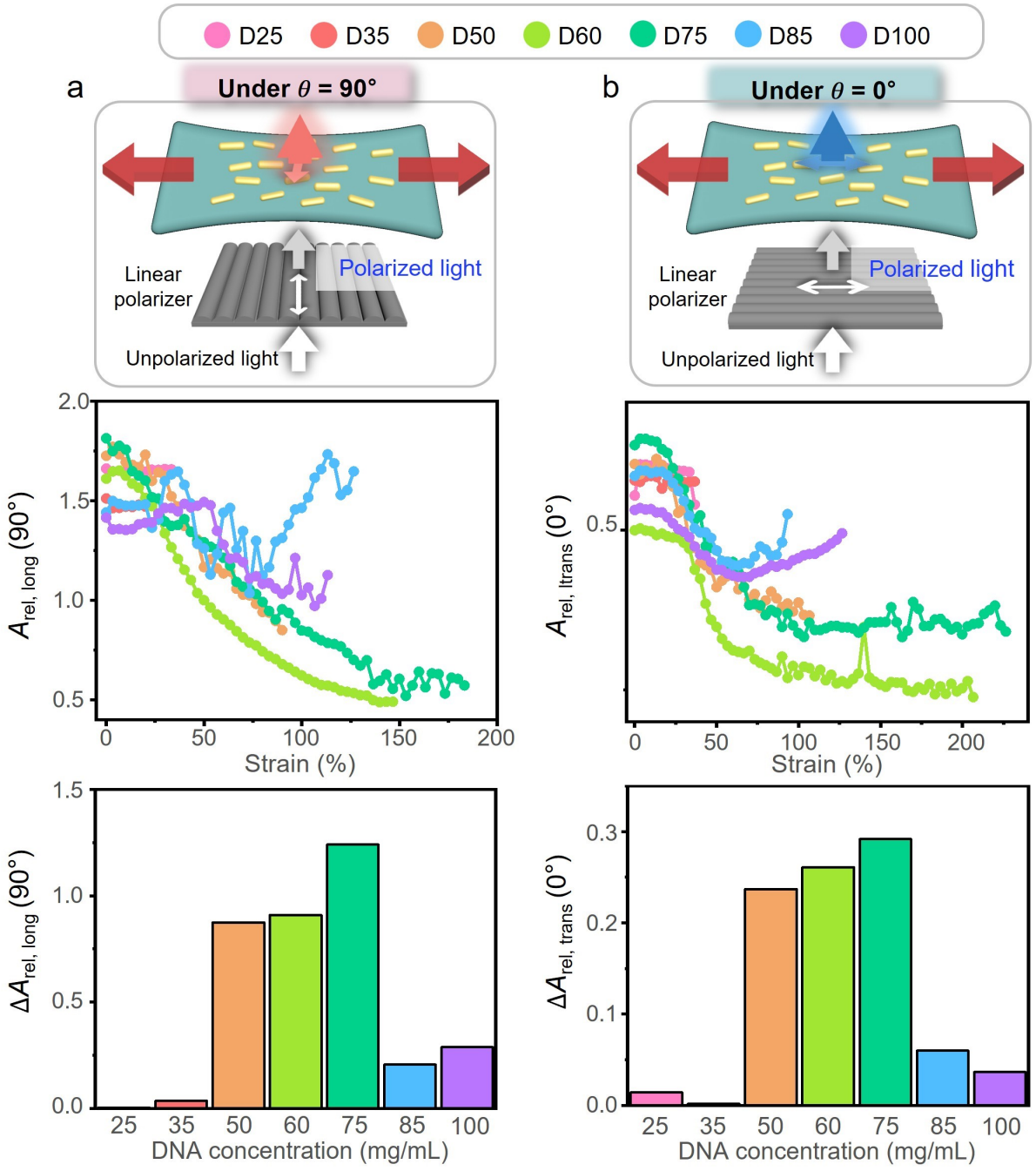

Fig. S15 Strain-dependent absorbance changes of DNA–GNR hydrogels under different polarization states and DNA concentrations. (a) Absorbance behavior under θ = 90°, where the incident light is polarized perpendicular to the stretching direction. (b) Absorbance behavior under θ = 0°, where the light is polarized parallel to the stretching direction. The top panels illustrate the experimental setup, showing the relative orientations of the polarizer and stretching axis. The middle panels display the relative absorbance (A_{rel}) as a function of applied strain for different DNA concentrations.The bottom panels compare the differential absorbance (ΔA_{rel}) for different DNA concentrations.

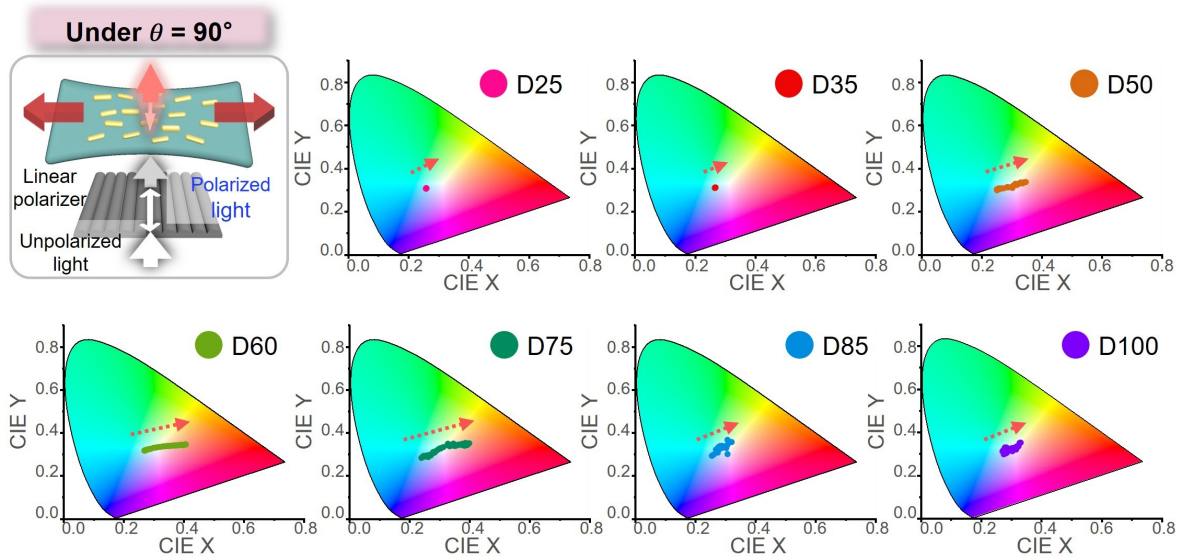

Fig. S16 CIE color coordinates of DNA–GNR hydrogels with varying DNA concentrations, measured under polarization perpendicular to the stretching direction (θ = 90°), showing the direction of plasmonic color shifts (red dashed arrows) with increasing mechanical strain.

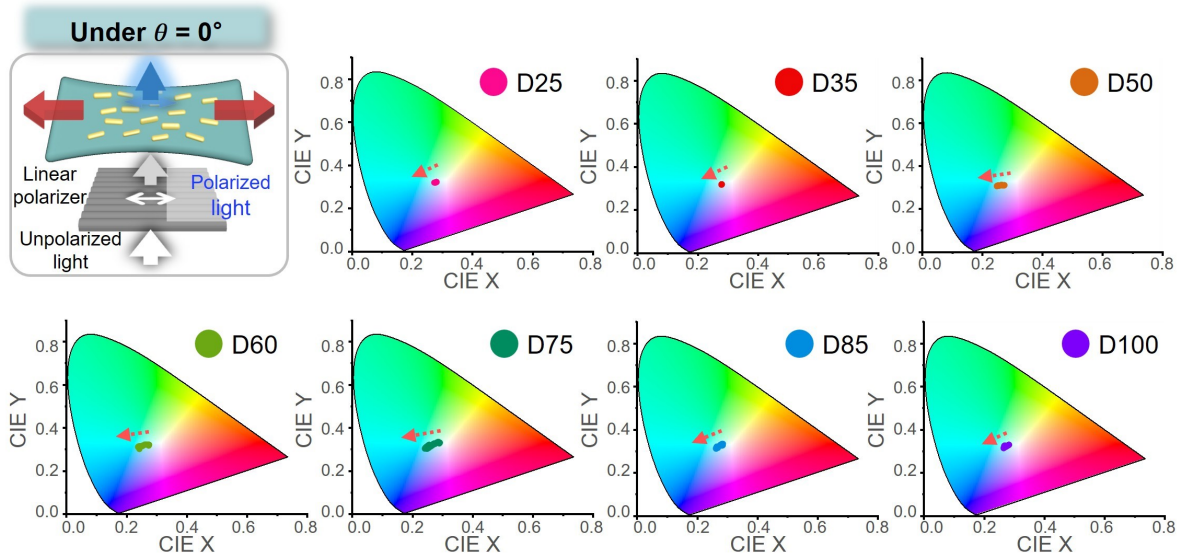

Fig. S17 CIE color coordinates of DNA–GNR hydrogels with varying DNA concentrations, measured under polarization parallel to the stretching direction (θ = 0°), showing the direction of plasmonic color shifts (red dashed arrows) with increasing mechanical strain.

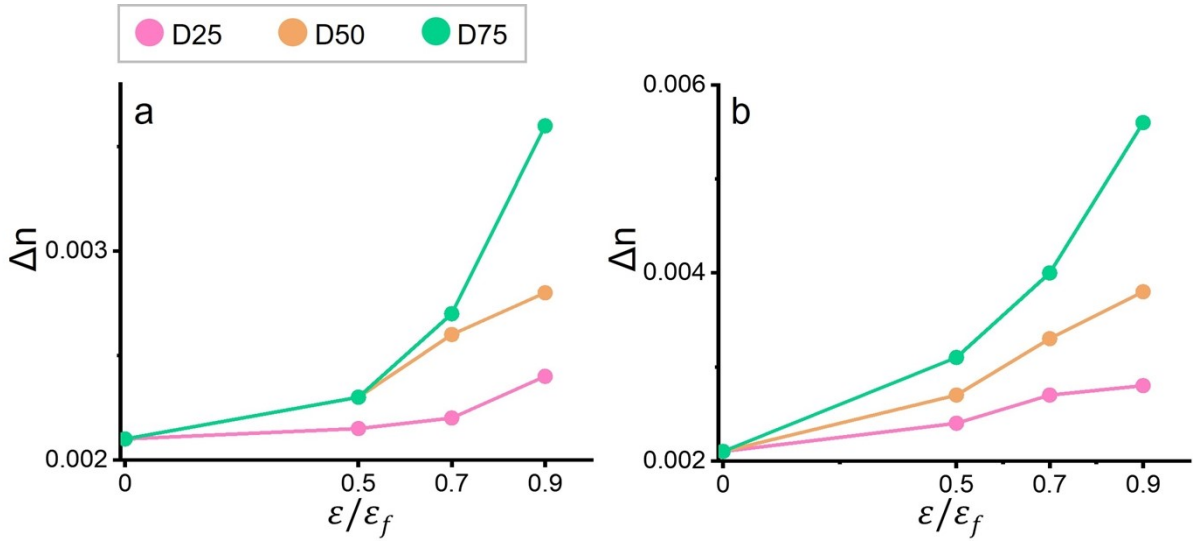

Fig. S18 Quantitative birefringence analysis of DNA hydrogels under uniaxial strain, based on chromatic shift comparison with the Michel–Levy chart. (a) Calculated birefringence assuming constant sample thickness (500 μm) across all strain levels. (b) Calculated birefringence accounting for strain-induced sample thinning under an assumption of isotropic shrinkage.

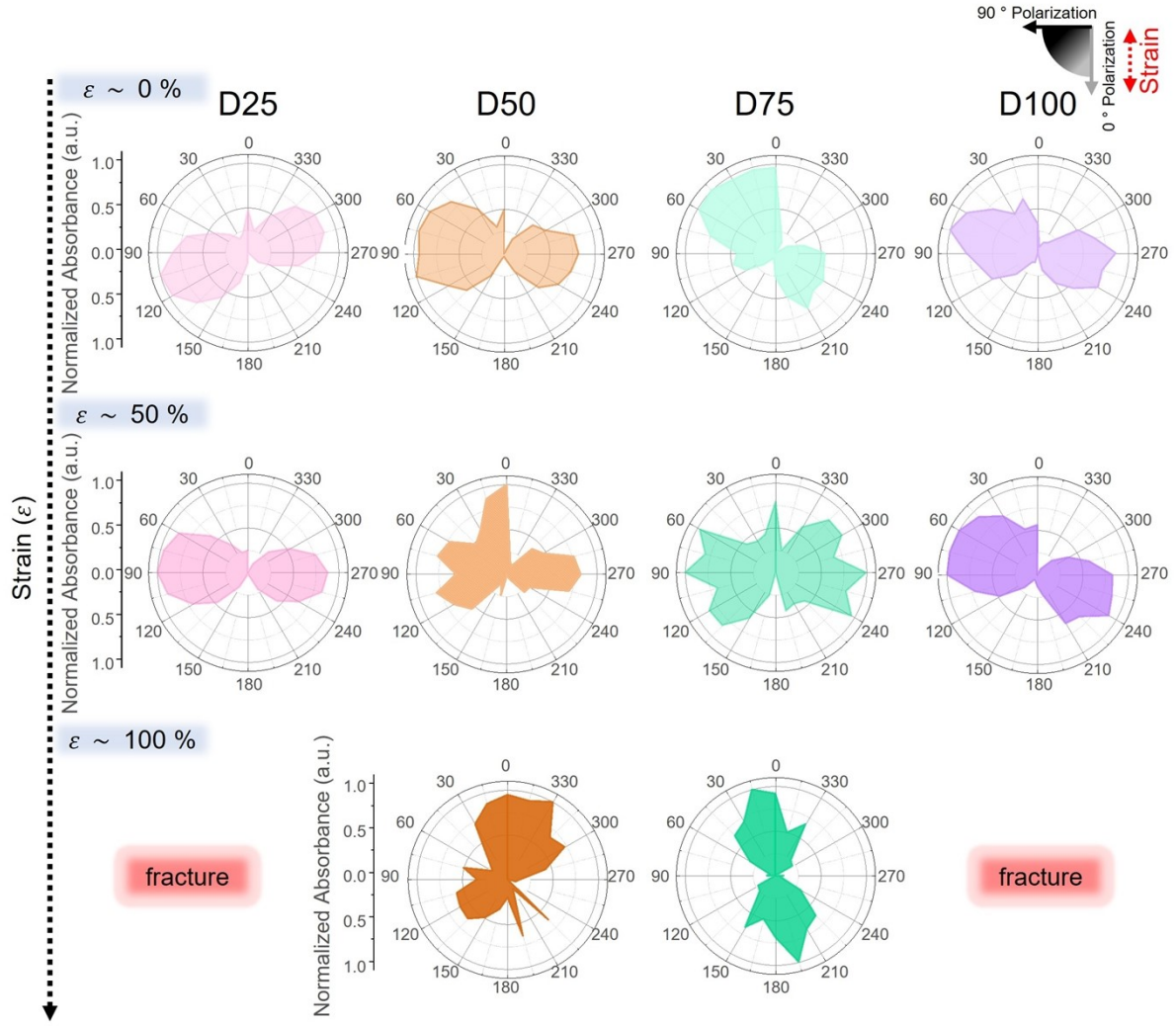

Fig. S19 Polar plots of normalized absorbance obtained from polarized FT-IR measurements of DNA–GNR hydrogels at various DNA concentrations and strain levels.

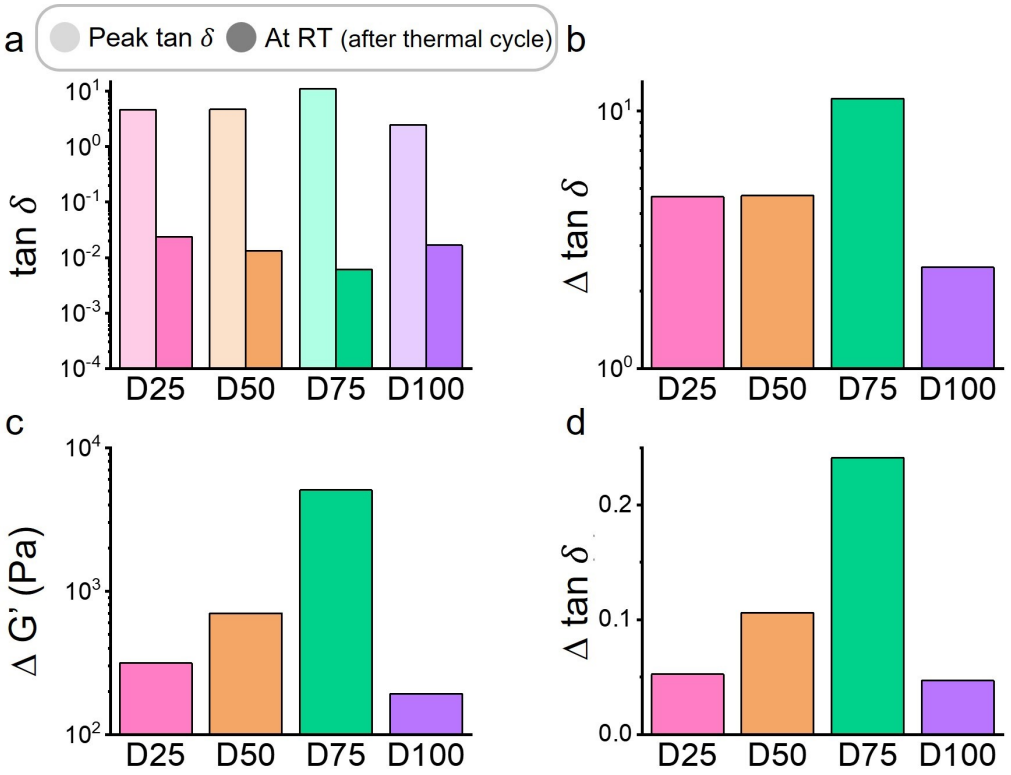

Fig. S20 Rheological property differences between solution and gel states. (a) Values of tan δ at peak temperatures during heating and after subsequent cooling to gel states, and (b) the corresponding differences (Δ tan δ) between these values. (c) Differences in storage modulus (G′) and (d) tan δ values between solution and gel states, measured at a frequency of 1 rad/s and temperature of 25 °C. The Y axes of tan δ are set as a log scale for (a) and (b) and a linear scale for (d), respectively, to allow for more effective comparison and enhancing clarity.